

# Superfluidity and BEC of liquid $^4\text{He}$ confined in a nanometer-size channel

著者 (英)	Junko Taniguchi, Rina Fujii, Masaru Suzuki
journal or publication title	Physical Review B
volume	84
number	13
page range	134511
year	2011-10-12
URL	<a href="http://id.nii.ac.jp/1438/00009288/">http://id.nii.ac.jp/1438/00009288/</a>

doi: 10.1103/PhysRevB.84.134511

# Superfluidity and BEC of liquid $^4\text{He}$ confined in a nanometer-size channel

Junko Taniguchi,\* Rina Fujii, and Masaru Suzuki

*Department of Engineering Science, University of Electro-Communications, Chofu, Tokyo 182-8585, Japan*

(Received 3 August 2011; published 12 October 2011)

We have studied the heat capacity and superfluidity of liquid  $^4\text{He}$  confined in a uniform and straight nanometer-size channel. The heat capacity of liquid  $^4\text{He}$  in the channel has a bend at a certain temperature  $T_B$ ; below this temperature a small amount of the superfluid fraction appears. This means that  $^4\text{He}$  atoms enter a BEC-like low-entropy state below  $T_B$ . Additionally, the superfluid fraction showed a second growth far below  $T_B$  under low pressure, accompanied by the dissipation. This two-stage growth is possibly a feature of the quasi-one-dimensional system.

DOI: [10.1103/PhysRevB.84.134511](https://doi.org/10.1103/PhysRevB.84.134511)

PACS number(s): 67.10.Ba, 67.25.de, 67.25.D-, 68.65.-k

## I. INTRODUCTION

Phase transitions of uniform bulk materials are drastically changed by a reduction in size. Over the past years, it has been widely noted that the transition temperature decreases for nanoparticles. The melting temperature in a 2-nm Au particle shifts to 500–600 K from 1337 K of its bulk value,<sup>1</sup> and the ferroelectric phase transition in a 2-nm  $\text{PbTiO}_3$  particle to 690 K from 770 K.<sup>2</sup> On the other hand, the introduction of disorder also changes the phase behavior. When a small amount of magnetic impurity is randomly substituted into metals, for example,  $\text{CuMn}$  or  $\text{AuFe}$ , a spin glass phase appears at low temperature, and the characteristic relaxation is observed.<sup>3</sup>

It is well known that the confinement of liquid  $^4\text{He}$  in porous media causes suppression of the superfluid transition by reducing the size.<sup>4</sup> Furthermore, the introduction of disorder due to porous media strongly affects the phase behavior. Recently, an anomalous superfluid behavior was observed for  $^4\text{He}$  in a Gelsil glass, which has an interconnected three-dimensional (3D) porous structure.<sup>5</sup> The superfluid onset temperature  $T_C$  is suppressed at 1.4 K under saturated vapor pressure (SVP), while the specific heat reaches maximum at a temperature higher than  $T_C$ .<sup>6</sup> This suggests that the separation between superfluidity and Bose-Einstein condensate (BEC) occurs in a Gelsil glass and that nanoscale BEC's are localized in pores.<sup>7</sup> The localized BEC state was also confirmed by a roton peak detected by neutron-scattering measurements.<sup>8</sup> In addition, under high pressure, the Bose glass phase was also observed.<sup>9</sup>

We have been studying the superfluid behavior of liquid  $^4\text{He}$  in a one-dimensional (1D) *uniform* nanochannel. It was found that the superfluid fraction grows rapidly at  $T_O$  (the rapid growth temperature) of about 0.9 K under 0.01 MPa,<sup>10</sup> and that this temperature is drastically suppressed from its bulk value of 2.17 K. It is of great interest to clarify the connection between superfluidity and BEC when the pore size is reduced without introduction of the disorder. Thus, we carried out heat capacity measurements for liquid  $^4\text{He}$  in the channel, and confirmed the superfluid fraction by comparison between  $\text{N}_2$ -filled and  $^4\text{He}$ -filled channels. From the present work, we found that the phase diagram of liquid  $^4\text{He}$  in a *uniform* nanochannel is qualitatively different from that of a Gelsil glass. Furthermore, a two-stage superfluid fraction growth was also found. This could be attributable to a feature of a quasi-1D system.

## II. EXPERIMENT

### A. Sample

The porous material FSM was synthesized by Inagaki *et al.* in Toyota Central R&D Laboratories, Inc., Japan.<sup>11</sup> It forms a honeycomb structure of a 1D uniform nanometer-size straight channel without interconnection. Using an organic molecule as a template, the diameter of the channel was precisely controlled. Its homogeneity was confirmed by transmission electron micrograph and the x-ray-diffraction pattern.<sup>12</sup> In the present work, we used the same batch of material as in previous work on torsional oscillator<sup>10</sup> and freezing pressure measurements.<sup>13</sup> The lattice constant of the honeycomb structure of FSM was 4.38 nm, and the 1D channel was 2.8 nm in diameter and 0.2–0.5  $\mu\text{m}$  in length. For heat capacity and torsional oscillator measurements, FSM powder was formed into pellets by mixing it with silver powder, as described in detail elsewhere.<sup>10,13</sup>

From the vapor pressure measurements,<sup>14</sup> it is known that about 70% of  $^4\text{He}$  atoms in the channel remain inert solid under SVP, and the effective diameter of liquid  $^4\text{He}$  is estimated as about 1.5 nm.

### B. Heat capacity measurement

The setup for heat capacity measurements is shown in Fig. 1. The pellet was put into a BeCu container  $\phi 13.0 \text{ mm} \times t 7.7 \text{ mm}$ . Surface area of the pellet was determined to be 182  $\text{mm}^2$  from Brunauer-Emmett-Teller fitting to the  $\text{N}_2$  adsorption isotherm, and the channel volume was estimated to be 138  $\text{mm}^3$  from the surface-volume ratio of FSM powder.<sup>12</sup> In the container, there were open spaces between FSM powders in the pellet, and between the pellet and the container.

The heat capacity was measured by a quasiadiabatic heat-pulse technique under pressure between 0.03 and 2.35 MPa. The temperature of the sample cell was monitored with  $\text{RuO}_2$  and Ge bare chip resistors, which were glued onto the bottom face of the cell. These were calibrated against a commercial calibrated  $\text{RuO}_2$  thermometer. On the top of the cell, a strain gauge with a resistance of 120  $\Omega$  (Ref. 15) was glued as a heater. Superconducting wires were used to reduce the heat current, and a superleak made of Vycor glass was inserted into the capillary to suppress the thermal conduction of bulk liquid  $^4\text{He}$  in the capillary. For the thermal isolation, the cell was supported from the isothermal copper stage only by a

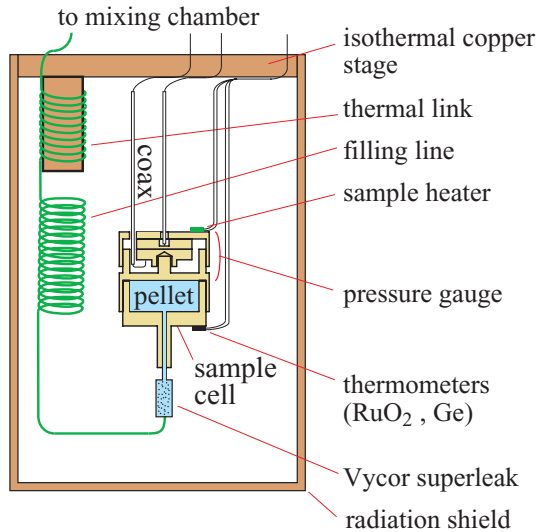


FIG. 1. (Color online) Schematic view of the experimental setup for heat capacity measurements.

filling capillary and was surrounded by a copper radiation shield. The stage was weakly linked to a mixing chamber of a dilution refrigerator. The thermal relaxation time from the cell to the stage was 180–5000 s, which was more than one order of magnitude larger than that in the cell, 10–120 s.

Figure 2 shows the total heat capacity of  $^4\text{He}$  under 0.03 MPa. The capacity has a sharp peak at  $T_\lambda$  of 2.16 K caused by the superfluid transition of bulk liquid  $^4\text{He}$  in the open spaces. We evaluated this amount by the method of Zassenhaus and Reppy.<sup>16</sup> In the inset, the capacity is replotted against the  $\log_{10}(|T - T_\lambda|/\text{K})$ . The bulk molar specific heat  $C_{\text{bulk}}$  is known to diverge at  $T_\lambda$  by the following equation:

$$C_{\text{bulk}} = \begin{cases} -A_0 \log_{10}(|T - T_\lambda|/\text{K}) + B_0 & (T < T_\lambda) \\ -A'_0 \log_{10}(|T - T_\lambda|/\text{K}) + B'_0 & (T > T_\lambda). \end{cases} \quad (1)$$

Here, the coefficients at 0.03 MPa were interpolated from molar specific heat data by Ahlers<sup>17</sup> and Okaji and Watanabe.<sup>18</sup>  $A_0 = 12.34 \text{ J/mol K}$  for  $T > T_\lambda$  and  $A'_0 = 11.72 \text{ J/mol K}$  for  $T < T_\lambda$ .

Comparing the divergence of the total heat capacity at  $T_\lambda$  with Eq. (1), we found that both the temperature dependence and the ratio of  $A_0/A'_0$  are well reproduced. From the magnitude of the divergence, we evaluated bulk liquid  $^4\text{He}$  in the open spaces as  $3.92 \pm 0.27 \text{ mmol}$ , and the corresponding volume was  $113 \pm 8 \text{ mm}^3$ .  $^4\text{He}$  in the channel, on the other hand, was estimated as 5.7 mmol from the total volume of the container.

For the entire temperature and pressure region, the heat capacity of bulk  $^4\text{He}$  in the open spaces was calculated using specific heat data by Brooks and Donnelly,<sup>19</sup> Ahlers,<sup>20</sup> and Lounasmaa.<sup>21</sup>

### C. Torsional oscillator measurement

The setup of torsional oscillator measurements was the same as in the previous work.<sup>10</sup> The oscillator consisted of a BeCu head containing the pellet and a BeCu hollow torsion. The surface area of the pellet was  $114 \text{ m}^2$ . The volumes

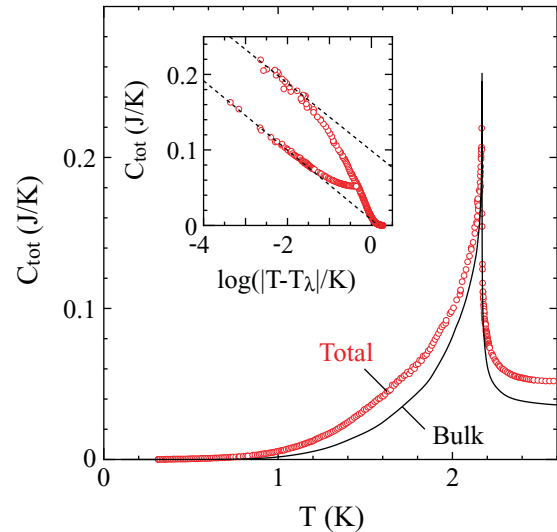


FIG. 2. (Color online) Total heat capacity of  $^4\text{He}$  in the cell under 0.03 MPa. The bulk liquid  $^4\text{He}$  contribution is represented by a solid curve. Inset: Total heat capacity against  $\log_{10}(|T - T_\lambda|/\text{K})$ .

of the 1D channel and the open spaces were  $86 \pm 4$  and  $35 \pm 4 \text{ mm}^3$ , respectively. The torsion head oscillates at a resonance frequency of 2.06 kHz with a high-quality factor of  $Q = 1.3 \times 10^6$  in vacuum at 4 K.

In the present work, we carried out torsional oscillator measurements of when the channel was filled with solid  $\text{N}_2$  ( $\text{N}_2$ -filled condition); under this condition, the superfluid fraction of bulk liquid  $^4\text{He}$  in the open spaces was observed. By subtracting this fraction from that of the previous measurements ( $^4\text{He}$ -filled condition), we could properly separate the contribution of the 1D channel.

For the  $\text{N}_2$ -filled condition,  $\text{N}_2$  gas was introduced into the sample cell at 77 K up to a pressure of 0.7 MPa, at which the channel was filled with liquid  $\text{N}_2$  due to the capillary condensation. To avoid blocking the filling line, the refrigerator was slowly cooled to 4.2 K. Compared with the empty cell, the resonance frequency dropped by 5 Hz, which was caused by filling the channel with solid  $\text{N}_2$ , while the  $Q$  factor remained.

## III. RESULTS

### A. Heat capacity

Figure 3 shows the heat capacity of  $^4\text{He}$  in the channel under various pressures below 2.35 MPa, together with 5.47 MPa at 0.3 K when  $^4\text{He}$  in the channel is solid at low temperature.<sup>22</sup> For clarity, the sets of data are shifted vertically by 0.005 J/K. The heat capacity of bulk liquid  $^4\text{He}$  in the open spaces was subtracted below 2.35 MPa, while that of bulk solid  $^4\text{He}$  was not for 5.47 MPa.

From the amount of liquid  $^4\text{He}$  in the channel, the molar specific heat was estimated to be about  $12 \text{ J/mol K}$  at around 2 K under 0.03 MPa.<sup>23</sup> This value is almost the same as bulk liquid  $^4\text{He}$  far above  $T_\lambda$ , and means that liquid  $^4\text{He}$  in the channel behaves as a classical fluid at high temperature. As the temperature is decreased, the heat capacity shows a clear bend at  $T_B$  (the bend temperature) of about 1.65 K under 0.03 MPa, and decreases rapidly below  $T_B$ . (Here, we define

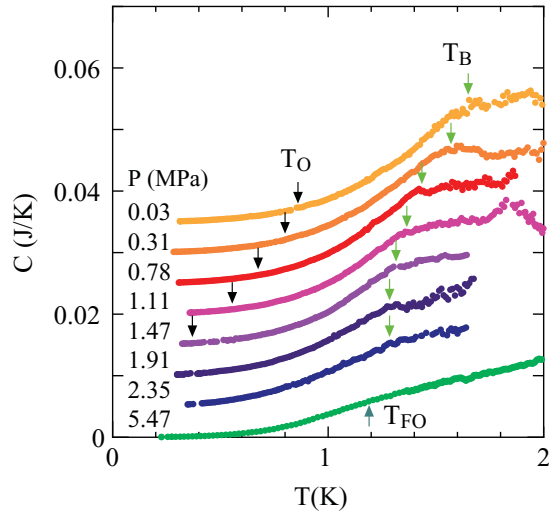


FIG. 3. (Color online) Heat capacity of  $^4\text{He}$  in the channel under various pressures. For clarity, the sets of data are shifted vertically. Solid downward arrows point to  $T_B$  (the bend temperature) and  $T_O$  (the rapid growth temperature).<sup>10</sup> An upward arrow points to  $T_{FO}$  (the freezing onset temperature).<sup>13</sup> Figures are the pressures at low temperature.

$T_B$  as the intersection of the extrapolation from both the high- and the low-temperature sides.) This behavior indicates that  $^4\text{He}$  atoms fall into a low-entropy state at  $T_B$ . In the previous work on torsional oscillator measurements, it was found that the superfluid fraction in the channel increases rapidly at  $T_O$  of 0.89 K (under 0.02 MPa). In the present experimental resolution, we observed no specific feature of the heat capacity.

As the pressure is increased, the magnitude of the heat capacity at high temperature becomes slightly less and  $T_B$  shifts to the low-temperature side. With further increasing pressure, the magnitude continues to decrease and the bend becomes obscure. On the other hand, the bend is indistinct for 5.47 MPa, at which the freezing onset occurs at  $T_{FO}$  of 1.19 K. It is interesting to examine the heat capacity of liquid  $^4\text{He}$  above the bulk freezing pressure of 2.53 MPa. We found, however, that it was difficult to determine whether the heat capacity has a bend, because of the additional heat capacity due to the freezing of bulk  $^4\text{He}$  in the open spaces.

### B. Superfluid fraction in the channel

Figure 4(a) shows the frequency shift from  $T_\lambda$  and the change in  $Q$  factor under 0.02 MPa for both the  $\text{N}_2$ -filled and  $^4\text{He}$ -filled conditions. For the  $\text{N}_2$ -filled condition, the frequency increases at  $T_\lambda$  due to the superfluid fraction in the open spaces. As the temperature is decreased, this increase decreases monotonously and the frequency approaches a constant value.

On the other hand, in the  $^4\text{He}$ -filled condition, the increase in frequency just below  $T_\lambda$  is in good agreement with that of the  $\text{N}_2$ -filled condition. However, it begins to deviate upward at about 1.65 K from that of the  $\text{N}_2$ -filled condition, and with further decrease in temperature, increases again rapidly at  $T_O$  of 0.89 K.

Regarding the  $Q$  factor,  $\Delta Q^{-1}$  has a break at  $T_\lambda$  under both conditions. For the  $\text{N}_2$ -filled condition, it decreases

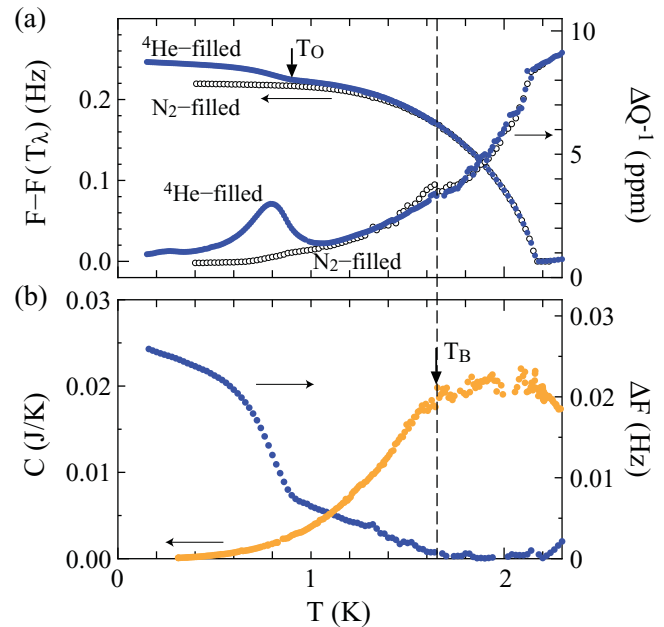


FIG. 4. (Color online) (a) Frequency shift from  $T_\lambda$ , and change in the  $Q$  factor. Solid and open symbols are for the  $^4\text{He}$ - and  $\text{N}_2$ -filled conditions under 0.02 MPa, respectively. (b) Difference of the frequency shift between  $^4\text{He}$ - and  $\text{N}_2$ -filled conditions, together with heat capacity of  $^4\text{He}$  in the channel under 0.03 MPa.

monotonously below this break, while in contrast, for the  $^4\text{He}$ -filled condition it increases below 1.05 K, and takes a maximum value at 0.79 K. Here, it should be noted that the temperature of the maximum value is not  $T_O$ , but almost coincides with that of the steepest increase in frequency below  $T_O$ . This suggests that this dissipation peak does not reflect the critical fluctuation due to the phase transition.

The difference in the frequency shift between the two conditions is plotted in Fig. 4(b). The superfluid fraction in the channel appears at  $T_B$ . With decreasing temperature, it linearly increases between  $T_B$  and  $T_O$ .<sup>24</sup> It then rises rapidly at  $T_O$ , and its increase becomes slow again at low temperature. In the previous work under the  $^4\text{He}$ -filled condition,<sup>10</sup>  $T_O$  was referred to as the superfluid onset in the channel. In the present work, however, it was made clear that the superfluid onset occurs not at  $T_O$ , but at  $T_B$ , and that the superfluid fraction increases again rapidly at  $T_O$ , i.e., the superfluid shows clear two-stage growth. Its magnitude at  $T_O$  is about one-third that at the lowest temperature. The temperature dependence is remarkably different from that of bulk  $^4\text{He}$ ; the fraction increases rapidly at  $T_\lambda$  and its increase becomes monotonously small with decreasing temperature.

Figure 5 shows the difference in frequency shift for several pressures between 0.02 and 2.36 MPa. For clarity, the sets of data are shifted by 0.005 Hz. The deviation in frequency shift always started at  $T_B$  although it was gradually suppressed to the low-temperature side with increasing pressure. This means that the superfluidity appears when  $^4\text{He}$  atoms fall into a low-entropy state without respect to pressure. The slope in the increase at  $T_B$  decreases weakly with increasing pressure. In contrast, the magnitude of the second growth is significantly

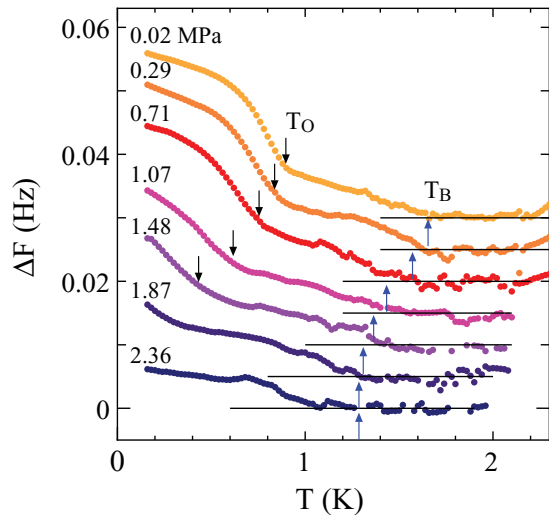


FIG. 5. (Color online) Difference of the frequency shift below  $T_\lambda$  between  $^4\text{He}$ - and  $\text{N}_2$ -filled conditions. For clarity, the sets of data are shifted vertically by 0.005 Hz. The downward and upward arrows show  $T_O$  and  $T_B$ , respectively. The horizontal lines are a guide for the eye.

suppressed with increasing pressure, and this growth is wiped out above about 2.1 MPa.

### C. Phase diagram

Figure 6 shows the the pressure-temperature phase diagram of superfluidity in the channel, together with the freezing onset curve. Here,  $T_B$  is the bend temperature of the heat capacity at which the superfluid onset occurs simultaneously,  $T_O$  is the rapid growth temperature of the superfluid fraction,<sup>10</sup> and  $T_{FO}$  is the freezing onset temperature.<sup>13</sup>

$T_B$  was found to have a weak pressure dependence at low pressure, while above 1.5 MPa was almost independent of pressure. On the other hand,  $T_O$  is decreased rapidly with

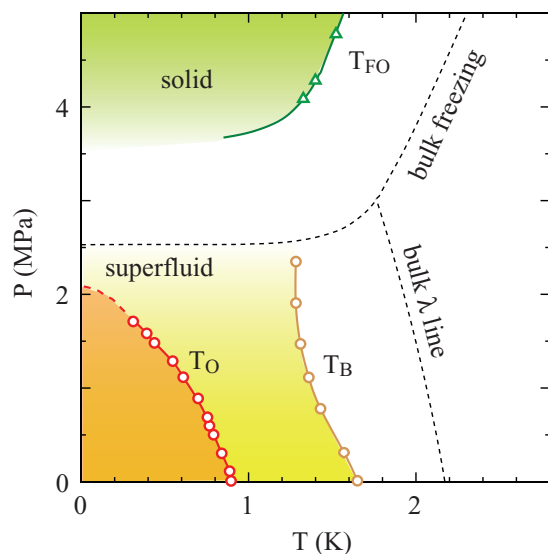


FIG. 6. (Color online) Pressure-temperature phase diagram of  $^4\text{He}$  in the channel. Solid circles:  $T_O$ , open circles:  $T_B$ , triangles:  $T_{FO}$ .

increasing pressure, and finally approaches zero at a pressure of about 2.1 MPa. This pressure is remarkably lower than the freezing pressure in the channel of 3.27–3.80 MPa at low temperature.<sup>13</sup> Furthermore, it should be noticed that  $T_O$  is not scaled by  $T_B$ , and that the magnitude of the second growth is not scaled by  $T_O$ .<sup>24</sup>

## IV. DISCUSSION

From the present work, we found that the superfluid onset of liquid  $^4\text{He}$  in the 1D channel occurs at the same time that  $^4\text{He}$  atoms enter a low-entropy state, probably BEC. This is in contrast to  $^4\text{He}$  in a Gelsil glass; the superfluid phase appears at a lower temperature than the localized BEC. The present medium, FSM, has a 1D uniform nanochannel without interconnection, while the Gelsil glass has a highly interconnected structure of nanopores. We speculate that the difference between FSM and Gelsil glass originates from the difference in the uniformity of nanopores, i.e., the separation between superfluidity and BEC results not from the reduction in size, but from the introduction of disorder.

It is interesting to examine the relation between the superfluid onset and the reduction in size. In the vicinity of  $T_\lambda$  for bulk liquid  $^4\text{He}$ , the superfluid onset temperature  $T_C$  of  $^4\text{He}$  confined in porous media is determined by comparison of the correlation length with the pore size, as  $(1 - T_C/T_\lambda) = (d/d_0)^{-1/\nu}$ , where  $d$  is the pore size and  $d_0$  is a constant. From experiments for the pore size larger than about 10 nm, it is known that  $\nu$  ranges between 0.65<sup>25,26</sup> and 0.67,<sup>27,28</sup> and  $d_0$  between 0.1 and 0.2 nm.<sup>29</sup> If we extend this relation to a smaller pore size,  $T_C$  for FSM is estimated as 1.58–1.82 K using the effective diameter of 1.5 nm. We found that the estimated value of  $T_C$  is in agreement with  $T_B$  of 1.73 K under 0.02 MPa.

Next we discuss the temperature dependence of the superfluid fraction. The remarkable feature of the 1D channel is a two-stage growth: Although the superfluid transition takes place at the same temperature  $T_B$  as a BEC-like low-entropy state, the fraction increases rapidly at a certain temperature  $T_O$ , accompanied by the dissipation. This is in contrast to bulk liquid  $^4\text{He}$ , in which the superfluid fraction increases monotonously below  $T_\lambda$ .

It should be noted that long-range phase coherence is not always necessary for the superfluid response for torsional oscillator measurements.<sup>30,31</sup> Recently, Eggel *et al.* calculated the momentum response function of a long 1D system.<sup>32</sup> They explained that the superfluid response occurs at low temperature because of the dynamical suppression of phase slips. Referring to their theoretical study, the observed temperature dependence of the superfluid fraction can be interpreted as follows: At  $T_B$ ,  $^4\text{He}$  atoms in the channel enter a BEC-like low-entropy state, and then they show the superfluid response with a *weak* long-range phase coherence. As the temperature decreases, the increase in superfluid fraction is observed because the dynamical response of phase slips is suppressed. According to this scenario, the rapid growth at low temperature is a dynamical effect. Therefore, it is of great importance to examine whether the rapid growth depends on frequency. This is a subject for future study.

Finally, we make a short comment on the temperature dependence of the superfluid fraction far below  $T_0$ . For bulk

liquid  $^4\text{He}$ , the change in the superfluid fraction is related to the specific heat of 3D phonons, and is in proportion to  $T^4$ . In the present work, the observed heat capacity is close to  $T^3$  between 0.3 and 0.7 K, and at the lower temperature there exists a  $T$ -linear term. From these facts, we might deduce the  $T^2$  or  $T^4$  dependence of the superfluid fraction. In contrast, the superfluid fraction shows a  $T$ -linear dependence, at least under low pressure, as shown in Fig. 5, suggesting that the mechanism of the temperature dependence is different from bulk liquid  $^4\text{He}$ . This remains an open question.

## V. SUMMARY

We have studied the heat capacity and the superfluidity of liquid  $^4\text{He}$  confined in a uniform and straight nanochannel. It

was found that the heat capacity of  $^4\text{He}$  in the channel has a bend at  $T_B$ . In addition, at the same temperature the superfluid fraction in the channel was observed. This demonstrates that  $^4\text{He}$  atoms enter a BEC-like low-entropy state below  $T_B$ . In contrast to bulk liquid  $^4\text{He}$ , the superfluid fraction shows clear two-stage growth under low pressure, accompanied by the dissipation. This two-stage growth is possibly a feature of the quasi-1D system.

## ACKNOWLEDGMENTS

This work was partly supported by a Grant-in-Aid for Scientific Research on Priority Areas, “Physics of Super-clean Materials” from the Ministry of Education, Culture, Sports, Science and Technology, Japan.

\*tany@phys.uec.ac.jp

<sup>1</sup>Ph. Buffat and J.-P. Borel, *Phys. Rev. A* **13**, 2287 (1976).

<sup>2</sup>K. Ishikawa, K. Yoshikawa, and N. Okada, *Phys. Rev. B* **37**, 5852 (1988).

<sup>3</sup>K. Binder and A. P. Young, *Rev. Mod. Phys.* **58**, 801 (1986).

<sup>4</sup>N. Wada, A. Inoue, H. Yano, and K. Torii, *Phys. Rev. B* **52**, 1167 (1995). See the references 24–28, 31.

<sup>5</sup>K. Yamamoto, H. Nakashima, Y. Shibayama, and K. Shirahama, *Phys. Rev. Lett.* **93**, 075302 (2004).

<sup>6</sup>K. Yamamoto, Y. Shibayama, and K. Shirahama, *Phys. Rev. Lett.* **100**, 195301 (2008).

<sup>7</sup>A. V. Lopatin and V. M. Vinokur, *Phys. Rev. Lett.* **88**, 235503 (2002).

<sup>8</sup>O. Plantevin, H. R. Glyde, B. Fak, J. Bossy, F. Albergamo, N. Mulders, and H. Schober, *Phys. Rev. B* **65**, 224505 (2002).

<sup>9</sup>J. Bossy, J. V. Pearce, H. Schober, and H. R. Glyde, *Phys. Rev. B* **78**, 224507 (2008).

<sup>10</sup>J. Taniguchi, Y. Aoki, and M. Suzuki, *Phys. Rev. B* **82**, 104509 (2010).

<sup>11</sup>S. Inagaki, Y. Fukushima, and K. Kuroda, *J. Chem. Soc. Chem. Commun.* **22**, 680 (1993).

<sup>12</sup>S. Inagaki, A. Koiwai, N. Suzuki, Y. Fukushima, and K. Kuroda, *Bull. Chem. Soc. Jpn.* **69**, 1449 (1996).

<sup>13</sup>J. Taniguchi and M. Suzuki, *Phys. Rev. B* **84**, 054511 (2011).

<sup>14</sup>H. Ikegami, T. Okuno, Y. Yamato, J. Taniguchi, N. Wada, S. Inagaki, and Y. Fukushima, *Phys. Rev. B* **68**, 092501 (2003).

<sup>15</sup>Kyowa Electronic Instruments Co. Ltd., Model number: KFL-02-0120-C1-16.

<sup>16</sup>G. M. Zassenhaus and J. D. Reppy, *Phys. Rev. Lett.* **83**, 4800 (1999).

<sup>17</sup>G. Ahlers, *Phys. Rev. A* **8**, 530 (1973).

<sup>18</sup>M. Okaji and T. Watanabe, *J. Low Temp. Phys.* **32**, 555 (1978).

<sup>19</sup>J. S. Brooks and R. J. Donnelly, *J. Phys. Chem. Ref. Data* **6**, 51 (1977).

<sup>20</sup>G. Ahlers, *Phys. Rev. A* **3**, 696 (1971).

<sup>21</sup>O. V. Lounasmaa, *Cryogenics* **1**, 212 (1961).

<sup>22</sup>J. Taniguchi, R. Fujii, and M. Suzuki, *J. Low Temp. Phys.* **162**, 544 (2010).

<sup>23</sup>Since 70% of  $^4\text{He}$  atoms in the channel remain inert solid under SVP, <sup>16</sup> the amount of liquid  $^4\text{He}$  is estimated as 1.6 mmol. We calculated the molar specific heat on the assumption that the contribution from inert solid is small.

<sup>24</sup> $T_O$  was determined by the intersection in resonance frequency of the extrapolation from the high temperature side and the steepest increase. With increasing pressure, the increase in frequency has a longer tail, and the decision of  $T_O$  is ambiguous. It was found, however, that  $T_O$  decreases in parallel with the dissipation peak, and it is reasonable that  $T_O$  is a measure of the second growth.

<sup>25</sup>G. G. Ihas and F. Pobel, *Phys. Rev. A* **9**, 1278 (1974).

<sup>26</sup>N. Giordano, *Phys. Rev. B* **27**, 5447 (1983).

<sup>27</sup>M. Kriss and I. Rudnick, *J. Low Temp. Phys.* **3**, 339 (1970).

<sup>28</sup>J. S. Brooks, B. B. Sabo, P. C. Schubert, and W. Zimmermann Jr., *Phys. Rev. B* **19**, 4524 (1979).

<sup>29</sup>C. W. Kiewiet, H. E. Hall, and J. D. Reppy, *Phys. Rev. Lett.* **35**, 1286 (1975).

<sup>30</sup>D. J. Bishop and J. D. Reppy, *Phys. Rev. Lett.* **40**, 1727 (1978).

<sup>31</sup>J. M. Kosterlitz and D. J. Thouless, in *Progress in Low Temperature Physics*, edited by D. F. Brewer (North-Holland, Amsterdam, 1978), Vol. 7B, p. 373.

<sup>32</sup>T. Eggel, M. A. Cazalilla, and M. Oshikawa, e-print arXiv:1104.0175v1.